FISEVIER

Contents lists available at ScienceDirect

### Materials Science and Engineering B

journal homepage: www.elsevier.com/locate/mseb



# Solid-phase crystallization kinetics and grain structure during thermal annealing of a-Si:H grown by chemical vapor deposition

S.P. Ahrenkiel<sup>a,\*</sup>, A.H. Mahan<sup>b</sup>, D.S. Ginley<sup>b</sup>, Y. Xu<sup>b</sup>

- a Nanoscience and Nanoengineering Department, South Dakota School of Mines and Technology, 501 E. Saint Joseph St., Rapid City, SD 57701, USA
- b National Center for Photovoltaics, National Renewable Energy Laboratory, 1617 Cole Blvd., Golden, CO 80401, USA

#### ARTICLE INFO

Article history: Received 4 January 2011 Received in revised form 28 March 2011 Accepted 2 May 2011

PACS: 61.05.-a

61.05.—a

61.66.Bi

61.72.uf

64.60.Q-64.70.dg

. .

Keywords: Hydrogenated amorphous silicon Annealing Crystallization kinetics Nucleation

Transmission electron microscopy

#### ABSTRACT

Solid-phase crystallization kinetics are examined during thermal annealing of as-deposited hydrogenated amorphous silicon (a-Si:H) thin films deposited by hot-wire chemical vapor deposition (HWCVD) and plasma-enhanced chemical vapor deposition (PECVD). The influence of deposition temperature of HWCVD material on crystallization is also considered. Real-time observation of the crystallization process using in situ transmission electron microscope heating allowed tracking of the crystalline volume fraction and grain number density by image-processing methods. Beyond an initial incubation period, roughly constant grain nucleation rate and growth velocity are observed. Extrapolation from early stages of crystallization allows estimation of the final average grain sizes. PECVD material shows a much lower nucleation rate than does HWCVD material under the same annealing conditions, whereas the grain growth velocities are comparable, leading to dramatically larger grain sizes in PECVD material. X-ray diffraction line widths from PECVD material are broader compared to HWCVD material. The diffraction line broadening is primarily determined by intragranular defect structure, rather than grain size. Low-temperature preannealing reduced the final XRD line widths of HWCVD material, indicating an influence on defect structure or density. Lattice contraction during crystallization of HWCVD material is observed to be independent of the initial hydrogen content.

© 2011 Elsevier B.V. All rights reserved.

#### 1. Introduction

Polycrystalline silicon (poly-Si) has great potential for largearea, thin-film applications, such as display technologies and photovoltaics, with greater stability than hydrogenated amorphous silicon (a-Si:H) [1]. Solar-cell production of poly-Si on glass produced by solid-phase crystallization is already in the commercial stage [2]. Hydrogen (H) passivation improves the transport properties of the poly-Si films, which are largely limited by grain-boundary recombination. Increasing grain sizes in these films has a corresponding, beneficial effect [3]. Similarly, methods to reduce the densities of intragranular defects are equally advantageous [4]. To this end, some investigators have focused on metal-catalyzed growth, or solid-phase epitaxy, using seeded or interfacial nucleation to generate large-grained material [5,6]. However, crystallization on amorphous substrates, particularly glass, via homogenous nucleation, is desirable because of its low

cost, inherent simplicity, and potential contribution to understanding the fundamental materials properties. Crystallization in these films occurs by spontaneous, homogeneous grain nucleation from an amorphous matrix and ensuing grain growth. In a-Si:H, an initial incubation period is sometimes observed before the onset of nucleation, during which the majority of the bonded hydrogen is released [7].

The initial H content of a-Si:H films increases as the growth temperature is decreased [8]. Whereas incorporated H is beneficial for the electronic properties of as-deposited a-Si:H, the continued presence of H during recrystallization may be less desirable. For example, increasing the initial hydrogen content has been shown to extend the total crystallization time [7,8]. After crystallization, material with initially high H levels also shows increased broadening of X-ray diffraction peaks [8]. Among the contributing factors may be grain size, defect density, or inhomogeneous strain. Therefore, microscopic determinations of grain size and grain morphology are needed to determine the structural manifestations of incorporated H.

Chemical vapor deposition (CVD) is a premier method to produce large-area films of a-Si:H with high throughput. Radio-frequency (RF) plasma-enhancement or hot-wire catalysis are used

<sup>\*</sup> Corresponding author. Tel.: +1 605 394 5238; fax: +1 605 394 2365. E-mail address: Phil.Ahrenkiel@sdsmt.edu (S.P. Ahrenkiel).

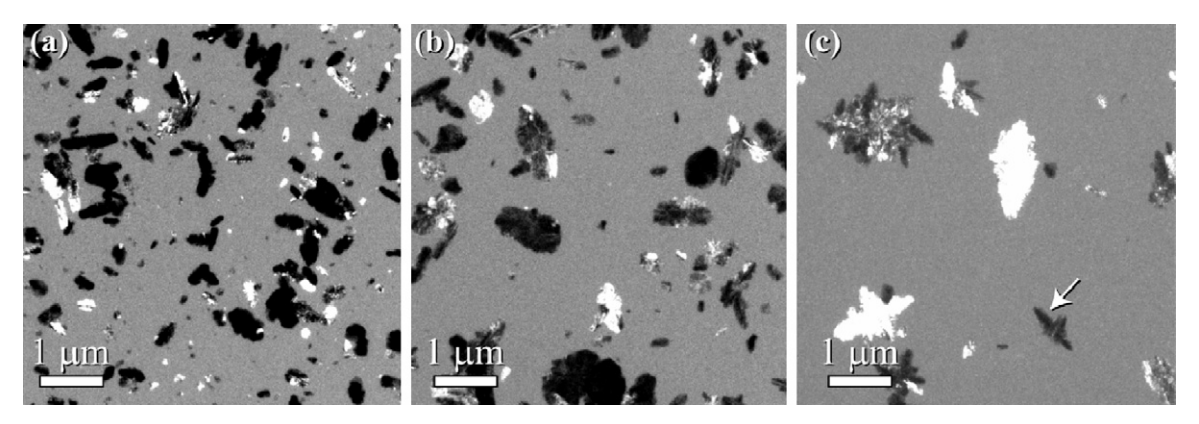


**Fig. 1.** TEM images of Si films partially crystallized after annealing at  $600^{\circ}$ C for various times: (a) low-H HWCVD (67 min); (b) high-H HWCVD (94 min); (c) PECVD (657 min). The crystalline volume fraction is roughly the same ( $X_c = 0.3$ ) in all three images. The arrow in (c) indicates a dendritic grain.

to create Si-H radicals from the flowing silane gas. Whereas the hotwire CVD (HWCVD) approach has been shown to produce better a-Si:H solar-cell devices in some cases [9], plasma-enhanced CVD (PECVD) is widespread and generally considered more scalable.

Numerous studies have examined microstructural characteristics of crystallized grains produced from a-Si films. Our goal in this work is a comparison of grain nucleation and grain growth kinetics of HWCVD and PECVD films analyzed by observation in transmission electron microscopy (TEM) using in situ heating. In combination with X-ray diffraction analysis, these results reveal several novel features of the crystallization in these materials.

#### 2. Experiment

Samples for X-ray diffraction were deposited on 1737 corning glass. Samples prepared specifically for TEM analysis were deposited directly on carbon (C)-coated, 200-mesh molybdenum TEM grids, by mounting the grids on glass using small drops of colloidal graphite paste on the edges of the grids. The grid manufacturers specify thicknesses of the C support films ranging from 3 to 20 nm.

HWCVD samples were grown at set points of  $250\,^{\circ}\text{C}$  and  $400\,^{\circ}\text{C}$ , at  $67\,\text{nm/min}$ , with a filament temperature of  $\sim\!2000\,^{\circ}\text{C}$ , and a silane flow rate of  $20\,\text{sccm}$  mixed with  $H_2$  at a pressure of  $20\,\text{Torr}$ . (Growth details are described elsewhere [10,11].) PECVD samples were grown at  $250\,^{\circ}\text{C}$  at  $10\,\text{nm/min}$  using a silane flow rate of  $30\,\text{sccm}$  at a pressure of  $550\,\text{mTorr}$  with  $0.5\,\text{W}$  of inductive power. In HWCVD, the H concentration has been previously shown to vary from approximately 11-12% at  $250\,^{\circ}\text{C}$  down to 2-3% at  $400\,^{\circ}\text{C}$  [8]. PECVD films grown at  $250\,^{\circ}\text{C}$ ,  $10\,\text{nm/min}$  are known to have H concentrations of 11-13% [8]. For this work, a standard, nominal thickness of  $1\,\mu\text{m}$  was used for films deposited on glass, whereas films deposited on TEM grids had a nominal thickness of  $100\,\text{nm}$ .

TEM analysis was performed on a CM 200 TEM operated at 200 kV using a Philips single-tilt holder and a Gatan Model 652 heating holder for in situ annealing. The heating holder uses a tantalum furnace, with a thermocouple that is spot welded to the furnace body. TEM images were acquired in conical dark-field mode, using an objective aperture with an approximate collection semi-angle of 4.4 mrad, positioned on the TEM optic axis. The direct beam was tilted by approximately 11.5 mrad and dynamically precessed about the optic axis, such that the diffracted 111, 220, and 311 beams contributed to the image. Post-growth annealing was also performed *ex situ* in a tube furnace with flowing N<sub>2</sub> gas.

Images were acquired with an Olympus KeenView 12-bit digital bottom-mount CCD camera. Software allowed automatic acquisition at regular intervals, typically 10 s. The images were corrected in post-acquisition processing with Gatan Digital Micrograph 3.4 software for camera artifacts using median filtering, and then aligned using cross correlation on recognizable, sub-image features. Iterative image matching was performed to precisely translate each image into registry with up to four preceding images.

Image processing of TEM images was used to determine the crystalline volume fraction,  $X_c$ . Two-dimensional grain structure is assumed, so that  $X_c = A_c/A$ , where  $A_c$  is the crystalline image area and A is the total image area. Images were binned into crystalline and amorphous regions by edge recognition, and then converted to one-bit black and white format. Computed histograms of the binary images were then used to evaluate  $X_c$ .

The grain number density  $\rho_g$  was determined by annotating the number of grains,  $N_g$ , visible within an area, A, of a TEM image, then computing  $\rho_g = N_g/A$ . To track grains in an image series, existing annotations were transferred to subsequent images, so that only inchoate nuclei needed to be identified.

X-ray diffraction (XRD) was performed using a Scintag X1 diffractometer with Cu-K $\alpha$  radiation. The instrumental line broadening was analyzed as a function of source and detector slit widths using a LaB $_6$  powder standard. Contributions to the instrumental broadening were found to arise from source divergence and detection optics. For peak-width analysis, the instrumental broadening was removed from the peaks by subtraction in quadrature. A Si powder standard was analyzed for comparison with the recrystallized a-Si:H films discussed here. Data was typically obtained only across the vicinities of known diffraction lines for c-Si powder in the diamond structure.

XRD peaks were fit in IGOR Pro software using Pearson-VII or pseudo-Voigt line shapes, with superposition of  $K\alpha_1$  and  $K\alpha_2$  contributions in the ratio 2:1 as functions of scattering vector, q, FWHM,  $\Delta q$ , and a shape parameter, m. Regardless of m, the various broadening contributions were assumed to combine in quadrature, (which holds precisely for a gaussian shape), allowing extraction of the intrinsic sample peak width for each reflection. The coincident 333/511 reflections were fit as a single peak.

#### 3. Results and discussion

TEM images of partially crystallized films show the coexistence of crystalline and amorphous phases. At roughly identical degrees of crystallization, distinct differences are apparent among low-H HWCVD, high-H HWCVD, and PECVD films (Fig. 1). Most apparent is a difference in grain size, with the smallest grains observed for low-H HWCVD films and the largest grains observed for PECVD films. Concomitantly, grains in the low-H HWCVD films typically appeared dense and featureless, whereas the PECVD films showed more irregular grains, often with dendritic, shape profiles.

#### Download English Version:

## https://daneshyari.com/en/article/1529968

Download Persian Version:

https://daneshyari.com/article/1529968

**Daneshyari.com**